Content-Adaptive Rain and Snow Removal Algorithms for Single Image

Shujian Yu[1,3(✉)], Yixiao Zhao[1,2(✉)], Yi Mou[3], Jinghui Wu[2], Lu Han[2], Xiaopeng Yang[2], and Baojun Zhao[2]

[1] Department of Electrical and Computer Engineering, University of Florida, Gainesville, USA
{yusjlcy9011,beng0429}@ufl.edu
[2] School of Information and Electronics, Beijing Institute of Technology, Beijing, China
zbj@bit.edu.cn
[3] Department of Electronics and Information Engineering,
Huazhong University of Science and Technology, Wuhan, China

Abstract. In this paper, we present two content-adaptive rain and snow removal algorithms for single image based on filtering. The first algorithm treats rain and snow removal task as an issue of bilateral filtering, where a content-based saliency prior is introduced. While the other views the same task from the perspective of guided-image-filtering, and the guidance image is derived according to the statistical property of raindrops or snowflakes as well as image background content. A comparative study and quantitative evaluation with some main existing image assessment algorithms demonstrate better performance of our proposed algorithms. The main contributions of our works are twofold: firstly, to the best of our knowledge, our algorithms are among the first to introduce image content information for single-image-based rain and snow removal; and secondly, we are also among the first to introduce quantitative assessment for single-image-based rain and snow removal tasks.

Keywords: Rain removal · Snow removal · Bilateral filtering · Guided-image-filtering · Outdoor vision

1 Introduction

Computer vision of indoor situations has already been extensively studied, whereas vision algorithms that can handle complex and unpredictable behaviors caused by different weather conditions, such as rain, snow, fog, or haze, in outdoor situations still remain as challenging problems [1].

Garg and Nayar [2] classified weather effects into two types: steady weather such as fog and haze, and dynamic weather such as rain and snow, based on the size of weather particles. In [3], an novel dehaze algorithm with dark channel prior was proposed, it achieves pretty good performance for removing steady weather effects.

However, for larger particles such as raindrops and snowflakes, reducing or removing the weather effects while preserving scene information is a different and difficult

Z. Zeng et al. (Eds.): ISNN 2014, LNCS 8866, pp. 439–448, 2014.
DOI: 10.1007/978-3-319-12436-0_49

task due to two main reasons: firstly, the visual appearance of raindrops or snowflakes depends both on their backgrounds and lighting conditions, which makes it difficult to build a general appearance model; and secondly, unlike steady weather conditions, rain and snow effects vary significantly over spatial and temporal domain [8].

Previous works for reducing the visibility of dynamic weather effects are primarily based on video, where physical and photometric properties of raindrops or snowflakes can be well employed over the whole video sequence [4-7]. Nevertheless, when only a single image is available, such as an image taken by a camera or downloaded from internet, algorithms for single-image-based rain/snow removal are essential.

Fu [8] proposed a rain streak removal diagram with image decomposition and morphological component analysis. This method assumes that rain streaks distributed homogeneously over the image. However, if the raindrops distributed heterogeneously and sparsely, it is difficult or impossible to learn a dictionary for rain streaks. Then, Xu [9] and Zheng [10] introduced guided-image-filtering [11] for rain/snow removal, where different refined guidance images are proposed separately. Both of the two algorithms ignored image content itself as well as statistical property of raindrops and snowflakes, and will inevitably introduce blurring artifacts to non-rain texture details.

In this paper, we propose two novel content-adaptive algorithms for single-image-based rain and snow removal. The first uses a content-based saliency a priori to segment original image, then different parts in resulting image correspond to regions with different perception intensity. Thus an easy but effective strategy is to adjust filter parameters adaptively. The other employs a guided-image-filtering based algorithm to remove rain and snow for single image, where the guidance image is derived from the statistical chromatic and the photometric properties of raindrops or snowflakes.

A comprehensive analysis is performed and quantitative comparison with two famous existing image assessment standards - visual information fidelity (VIF) metric [12] and feature-similarity (FSIM) index [13] are also carried out. Experimental results demonstrate the effectiveness and efficiency of our proposed algorithms.

The remainder of this paper is organized as followings: in section II and III, the details of our proposed two algorithms - bilateral filtering based algorithm with saliency a prior and guided-image-filtering based algorithm with statistical property are well explained; then in section IV, a comprehensive comparison analysis and quantitative evaluation is conducted; finally, section V concludes this paper.

2 Preliminary Knowledge

The intensity of rain and snow generally falls into four categories - light, moderate, heavy and violent (Fig. 1) - based on the rate of precipitation [14]. For images contaminated by raindrops or snowflakes with light or moderate intensity, it is difficult or impossible to learn a construction model accurately due to lack of useful information provided by single image as well as their sparse distribution and random directions. If images are contaminated with weather effects of heavy or violent intensity, although

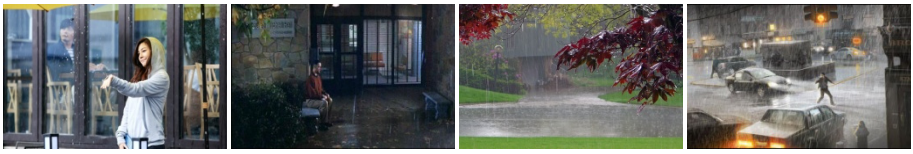

Fig. 1. The visual appearances of rain under different intensities. From left to right: (a) a beautiful girl in light rain; (b) a sitting man in moderate rain; (c) a building in heavy rain; and (d) crossroads in violent rain.

we can coarsely separate weather effects from background via dictionary learning and sparse coding [8], details in background (especially edges and corners resembling rain streaks or snowflakes) are often eliminated at the same time, only for the reason that raindrops or snowflakes are highly mixed with similar texture in almost each patch of the image. Therefore, unlike conventional image restoration problems, single-image-based rain/snow removal is not an easy and trivial task. However, algorithms based on edge-preserving filtering [11,15] provide a reliable solution.

2.1 Bilateral Filtering

As a simple, non-iterative scheme for edge-preserving smoothing, bilateral filtering is always the first step of computer vision based algorithms for different systems, such as vehicle tracking system, pedestrian detection and surveillance system [8], under rain or snow weather conditions. The basic idea of bilateral filtering is Gaussian distribution based averaging, which means that the intensity value at each pixel in an image is replaced by a weighted average of intensity values from nearby pixels [15]. However, the weights depend not only on Euclidean distance but also on the color intensity differences. This preserves sharp edges by systematically looping through each pixel and adjusting weights to the adjacent pixels accordingly [11].

2.2 Guided Image Filtering

In [11], He proposed a novel explicit image filter called guided filter. Derived from a local linear model, the guided filter computes the filtering output I_{guide} by considering the content of guidance image I, which can be the input image itself or another different image. In window ω_k, the output pixel q_i can be represented as:

$$q_i = a_k I_i + b_k, \forall i \epsilon \omega_k \tag{1}$$

where a_k and b_k are defined as:

$$a_k = ((\Sigma_{i\in\omega_k} I_i p_i)/|\omega| - u_k \overline{p_k})/(\sigma_k^2 + \varepsilon) \tag{2}$$

$$b_k = \overline{p_k} - a_k u_k \tag{3}$$

Here, p is the filter input, u_k and σ_k^2 are the mean and variance of I in ω_k, $\overline{p_k}$ is the mean of p in ω_k, $|\omega|$ is the pixel number in ω_k.

3 Bilateral Filtering Based Rain/Snow Removal with a Saliency Prior

According to aforementioned description in section II, as a widely used method for rain and snow removal for single image, conventional bilateral filtering has two major drawbacks: firstly, it will produce staircase effects at edges, especially at contours of un-degraded objects, and secondly, the filter parameters remain the same for all parts of the image without any emphasis, which will introduce similar blurring effects or flatting performance to both dominant objects and redundant backgrounds.

However, different parts of an image will cause different perception intensities to an observer: the salient parts, which always corresponding to dominant objects that are less influenced by raindrops or snowflakes, will lead to more perception intensity, whereas the less salient parts, which always corresponding to backgrounds or redundant image content, will result in low perception intensity. Therefore, it is essential to adaptively adjust filter parameters based on image content, i.e. content-aware saliency information in an image.

3.1 Content-Based Saliency Detection

Normally, raindrops or snowflakes result in low perception intensity compared with prominent objects in an image, due to the fact that such weather effects are always highly mixed with backgrounds and sparsely distributed.

In this section, we successfully introduce a saliency a priori for bilateral filtering. Different from the conventional bilateral filtering, our method can adaptively adjust filter parameters based on the intensity of saliency.

For the computation of saliency map, we use context-aware method [17] proposed by Goferman as our pre-processing step. The literatures on saliency detection contain nearly 65 vision attention models in the last 25 years [16], and we explain here why context-aware method is selected. Firstly, note that we have emphasized content-adaptive in this paper, and therefore methods designed for saliency detection only for dominant objects, regardless of surrounding context information, such as spectral residual approach [18] and global contrast based method [19], fall outside the scope of this paper. Secondly, of the existing methods for content-based saliency detection, methods based on symmetric surround or combined features introduced in [20] appear to be the closest in spirit to the context-aware saliency detection utilized here. However, only limited principles of human visual attention from psychology are utilized in [20], whereas [17] realized all of them mathematically. Fig. 2 demonstrates the saliency detection results.

(a) (b) (c) (d)

Fig. 2. Ground-truth images with rain/snow and their corresponding saliency map

3.2 Ordered Sample Clustering for Histogram of Saliency Map

For the saliency map from section 3.1, larger pixel values represent high salient regions of the original image, while smaller ones correspond to low salient regions.

With ordered sample clustering algorithm, the histogram of saliency map can be partitioned into several segments, and each segment represents a specific saliency intensity level. In this paper, we used the well-known "optimal partition method (i.e. fisher method)" to separate the image histogram into several segments. The basic idea of "optimal partition" is minimizing the increment of sum of deviation squares of the ordered sample after segmentation.

Fig. 3(a) illustrates the clustering result for saliency map histogram of Fig. 2(b) (clustered into 3 categories). Fig. 3(b) illustrates the image segmentation of Fig. 2(a) according to clustering result, each segmented region corresponding to a specific segment of histogram of saliency map.

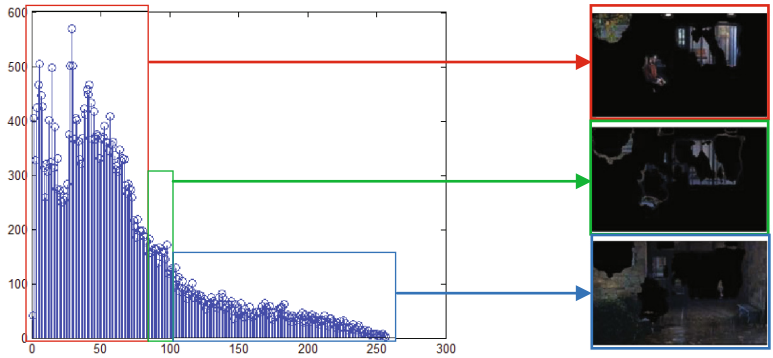

Fig. 3. Image segmentation according to ordered sample clustering to histogram of saliency map. (a) is the histogram of saliency map, the two breaking points are 75 and 101. (b) is image segmentation results.

3.3 Adaptive Parameter Adjustment

The performance of bilateral filtering depends on three parameters: filter width, standard deviations of geometric spread and photometric spread. The geometric spread σ_d controls the extent of low-pass filtering: a large value blurs more, and vice versa. Similarly, the photometric spread σ_r in the image range is set to achieve the desired amount of combination of pixel values. Therefore, it is reliable to allocate smaller filter parameters in the regions of high saliency, while in the low salient regions, larger parameters are preferable.

In our experiment, initial values for these three parameters, i.e. filter half-width, σ_d, and σ_r are set as 5, 3, and 0.1, respectively. For regions of lower saliency in the next level, we will increase each parameter by 2, 5, and 5 times, separately. The results are shown in Fig.4. Compared with conventional bilateral filtering method, our algorithm can preserve more image-related information (content) and remove raindrops and snowflakes with higher accuracy.

Fig. 4. Weather removal results for Fig. 3(a) and Fig.3(c) with refined bilateral filtering

4 Guided-Image-Filtering Based Rain/Snow Removal with Statistical Chromatic Property

Guided-image-filtering achieved good performance for dehaze. After that, feasible and practical extensions have been applied towards rain and snow removal [9,10]. Conventional revised guided-image-filtering algorithms are all based on the principle to preserve more useful details, especially edges. Here, we present a new method to extract guidance image based on statistical properties of raindrops/snowflakes.

4.1 Chromatic Property of Raindrops and Snowflakes

In [4], a chromatic model for spherical raindrop is presented (also applicable for snowflakes). It pointed out that raindrop refracts a wide range of light, therefore the projection of raindrop in the image is much brighter than its background. Because of the difference in wavelength, blue light has a larger index of refraction and a wider field of view than red light. Therefore, a raindrop should refract a little more blue light coming from the background. Followed with [2,4], we further investigated the subtle difference of refraction to the appearance of raindrops and snowflakes. According to our statistical observations[1], the intensity differences of R, G, and B channel caused by raindrops/snowflakes are roughly the same.

4.2 Photometric Property of Raindrops and Snowflakes

When a falling raindrop or a snowflake is captured by a camera, the intensity is a linear combination of irradiance of raindrops or snowflakes and the irradiance of background [9]. Their intensity values can be both expressed as:

$$I_{rs} = \int_0^{\tau} \overline{E_{rs}}\, dt + \iint_{\tau}^{T} \overline{E_b} dt \tag{4}$$

where I_{rs} is the intensity value of a pixel effected by raindrops or snowflakes, $\overline{E_{rs}}$ is the time-averaged irradiance of a stationary raindrop or snowflake, $\overline{E_b}$ is the time-averaged irradiance of background, T is the exposure time and during the time τ a raindrop or a snowflake is passing through the pixel.

[1] We verified these observations using two public videos from [21]. In each frame from the two videos, a fixed region of 50*50 is selected, and our observations are based on these 2500 pixel sequences.

If we define I_b as the background intensity, I_E as the intensity of a stationary raindrops or snowflakes at the time T. Eq.(4) can be simplified as:

$$I_{rs} = \alpha I_E + (1-\alpha) I_b, \text{where } \alpha = \tau / T \tag{5}$$

Eq.(5) provides a photometric model of raindrops and snowflakes.

4.3 Refined Guidance Image Extraction

Here, we proposed a new method for guidance image extraction based on both chromatic and photometric properties of raindrops or snowflakes. Firstly, extraction of guidance image can be achieved through following procedures:

I. Smooth input image with bilateral filtering in R, G, B channels separately. The result images can be represented as I_{bf_R}, I_{bf_G} and I_{bf_B}, respectively.

II. Compute abstract differential images between three images from step I. Then we have three difference images: I_{R-G}, I_{G-B} and I_{B-R}.

III. Use Eq.(6) to compute the mean image of I_{R-G}, I_{G-B} and I_{B-R}, I_{mean} can be used as our first refined guided image.

$$I_{mean} = (I_{R-G} + I_{G-B} + I_{B-R})/3 \tag{6}$$

In addition, we note that Eq.(5) is established for R, G and B channels. If C indicates a coordinate of the RGB space and I_{rs-C} is the maximum value at RGB space of I_{rs}, I_{b-C} must be the maximum value at RGB space of I_b. This relation also holds for the minimum value of each vector at RGB space. Therefore, we have:

$$I_{rs-max} = \alpha I_{E-max} + (1-\alpha) I_{b-max} \tag{7}$$

$$I_{rs-min} = \alpha I_{E-min} + (1-\alpha) I_{b-min} \tag{8}$$

According to aforementioned description $I_{E-max} = I_{E-min}$. Subtract (8) from (7):

$$I_f = I_{rs-max} - I_{rs-min} = (1-\alpha)(I_{b-max} - I_{b-min}) \tag{9}$$

Fig. 5. Raindrops/Snowflakes removal results with guided image filtering: first row shows removal reuslt for sitting man in rain weather; secod row shows removal result for mailbox in snow weather. From left to right: I_f, I_{mean}, $I_{guidance}$ and weather removal result.

Obviously, I_f is not affected by weather effects. Therefore, final guidance image $I_{guidance}$ can be represented as weighted combination of I_{mean} and I_f (See Fig.5):

$$I_{guidance} = \beta I_{mean} + (1 - \beta) I_f \tag{10}$$

5 Experiment and Result Analysis

We have conducted both qualitative and quantitative experiments to assess our proposed two algorithms with other state-of-art raindrop/snowflake removal algorithms. The goal of objective image quality assessment research is to provide computational models that can automatically predict perceptual image quality. In this paper, we will utilize VIF [12] and FSIM [13] to assess our raindrops/snowflakes removal results.

5.1 Qualitative Comparison

Fig.6 shows the weather effects removal results of several different filtering based methods[2]. The top row illustrates removal effects for raindrops, and the bottom row illustrates removal effects for snowflakes[3]. As can be seen, "GF" has good performance for rain/snow removal, but it introduces more blurring artificial effects. "BF" can keep more detail information, but it always preserve more weather effects. Compared with these two, "Xu" can keep more useful structure information, "Our I" can also keep more useful details and remove more weather effects. In addition, "Our II" outperforms "GF".

(a) (b) (c) (d) (e)

Fig. 6. Illustration of weather effects removal results with different algorithms: (a-e) removal results with "BF", "GF", "Xu", "Our I" and "Our II", respectively.

5.2 Quantitative Evaluation

In this section, VIF and FSIM are utilized to evaluate the raindrops and snowflakes removal effects quantitatively. Test images (See Fig.7) are downloaded from [21], where weather effects are added to the ground truth video frames with advanced rendering techniques [5]. Experimental results are presented in Table 1 and Table 2.

[2] More results are available from the author's homepage http://www.yushujian.com/index.html.

[3] We denote bilateral filtering in [15] as BF, guided-image-filtering in [11] as GF, Xu's method in [9] as Xu, our two proposed algorithm as Our I and Our II in section 5.1 and section 5.2.

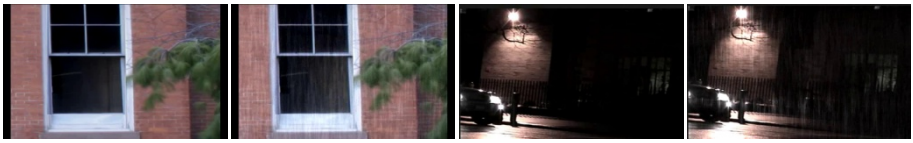

(a) (b) (c) (d)

Fig. 7. Two representative frames from two test videos: (a) and (c) are ground-truth images; (b) and (d) are ground-truth images with added weather effects

Table 1. Averaged VIF value for video frames with different algorithms

	BF	GF	Xu	Our I	Our II
Video I	0.1444	0.1172	0.1463	**0.1562**	0.1484
Video II	0.5378	0.5193	0.4463	**0.6477**	0.5745

Table 2. Averaged FSIM value for video frames with different algorithms

	BF	GF	Xu	Our I	Our II
Video I	0.3219	0.3039	0.3218	0.3302	**0.3360**
Video II	0.8180	0.7717	0.7553	**0.8395**	0.8119

6 Conclusion

In this paper, we have proposed two independent algorithms for raindrops/snowflakes removal in single image. Firstly, we successfully introduced a saliency-map-prior for bilateral filtering, the improved algorithm can automatically adjust filter parameters based on image content. In addition, we have also proposed a novel way for guidance image extraction based on properties of rain. The refined guided image filtering can achieve better performance than conventional version. Finally, we have conducted experiments to assess different rain streak removal methods both from subjective perspective and objective measurements. Experimental results demonstrate the effectiveness and efficiency of our proposed algorithms.

References

1. Zhang, X., Li, H., Qi, Y., Leow, W.K., Ng, T.K.: Rain Removal in Video by Combining Temporal and Chromatic Properties. In: Proceedings of the IEEE International Conference on Multimedia and Expo, pp. 461–464 (2006)
2. Garg, K., Nayar, S.K.: Detection and Removal of Rain from Videos. In: Proceedings of the IEEE Computer Society Conference on Computer Vision and Pattern Recognition, vol. 1, pp. I-528–I-535 (2004)
3. He, K., Sun, J., Tang, X.: Single Image Haze Removal Using Dark Channel Prior. IEEE Trans. Pattern Analysis and Machine Intelligence **33**(12), 2341–2353 (2011)
4. Garg, K., Nayar, S.K.: Vision and Rain. International Journal of Computer Vision **75**(1), 3–27 (2007)

5. Garg, K., Nayar, S.K.: Photorealistic rendering of rain streaks. ACM Transactions on Graphics (TOG) **25**(3), 996–1002 (2006)
6. Brewer, N., Liu, N.: Using the shape characteristics of rain to identify and remove rain from video. In: da Vitoria Lobo, N., Kasparis, T., Roli, F., Kwok, J.T., Georgiopoulos, M., Anagnostopoulos, G.C., Loog, M. (eds.) SSPR&SPR 2008. LNCS, vol. 5342, pp. 451–458. Springer, Heidelberg (2008)
7. Bossu, J., Hautière, N., Tarel, J.P.: Rain or snow detection in image sequences through use of a histogram of orientation of streaks. International Journal of Computer Vision **93**(3), 348–367 (2011)
8. Fu, Y.H., Kang, L.W., Lin, C.W., Hsu, C.T.: Single-frame-based rain removal via image decomposition. In: IEEE International Conference on Acoustics, Speech and Signal Processing (ICASSP), pp. 1453–1456 (2011)
9. Xu, J., Zhao, W., Liu, P., Tang, X.: An Improved Guidance Image Based Method to Remove Rain and Snow in a Single Image. Computer and Information Science **5**(3), 49 (2012)
10. Zheng, X., Liao, Y., Guo, W., Fu, X., Ding, X.: Single-Image-Based Rain and Snow Removal Using Multi-guided Filter. In: Lee, M., Hirose, A., Hou, Z.-G., Kil, R.M. (eds.) ICONIP 2013, Part III. LNCS, vol. 8228, pp. 258–265. Springer, Heidelberg (2013)
11. He, K., Sun, J., Tang, X.: Guided image filtering. In: Daniilidis, K., Maragos, P., Paragios, N. (eds.) ECCV 2010, Part I. LNCS, vol. 6311, pp. 1–14. Springer, Heidelberg (2010)
12. Sheikh, H.R., Bovik, A.C.: Image information and visual quality. IEEE Trans. Image Processing **15**(2), 430–444 (2006)
13. Zhang, L., Zhang, D., Mou, X.: FSIM: a feature similarity index for image quality assessment. IEEE Trans. Image Processing **20**(8), 2378–2386 (2011)
14. Glickman, T.S., Zenk, W.: Glossary of meteorology (2000)
15. Tomasi, C., Manduchi, R.: Bilateral filtering for gray and color images. In: International Conference on Computer Vision, pp. 839–846 (1998)
16. Borji, A., Itti, L.: State-of-the-art in visual attention modeling. IEEE Trans. Pattern Analysis and Machine Intelligence **35**(1), 185–207 (2013)
17. Goferman, S., Zelnik-Manor, L., Tal, A.: Context-aware saliency detection. IEEE Trans. Pattern Analysis and Machine Intelligence **34**(10), 1915–1926 (2012)
18. Hou, X., Zhang, L.: Saliency detection: A spectral residual approach. In: Proceedings of IEEE Conference on Computer Vision and Pattern Recognition (CVPR), pp. 1–8 (2007)
19. Cheng, M.M., Zhang, G.X., Mitra, N.J., Huang, X., Hu, S.M.: Global contrast based salient region detection. In: Proceedings of IEEE Conference on Computer Vision and Pattern Recognition (CVPR), pp. 409–416 (2011)
20. Liu, T., Yuan, Z., Sun, J., Wang, J., Zheng, N., Shum, H.: Y: Learning to detect a salient object. IEEE Trans. Pattern Analysis and Machine Intelligence **33**(2), 353–367 (2011)
21. Columbia University Computer Vision Laboratory Detection and Removal of Rain Project. http://www.cs.columbia.edu/CAVE/projects/rain_detection/